

HIGHER GENUS MAXFACES WITH ENNEPER END

RIVU BARDHAN, INDRANIL BISWAS, AND PRADIP KUMAR

ABSTRACT. We have proven the existence of new higher-genus maxfaces with Enneper-type end. These maxfaces are not the companions of any existing minimal surfaces, and furthermore, the singularity set is located away from the ends. The method for discovering these maxfaces involves utilizing the calculus of Teichmüller space, as proposed by Weber and Wolf in the case of minimal surfaces.

1. INTRODUCTION

Analogous to minimal surfaces in \mathbb{R}^3 , maximal surfaces are immersions with zero mean curvature in the Lorentz Minkowski space \mathbb{E}^3_1 . These surfaces arise as solutions to the variational problem of locally maximizing the area among space-like surfaces. There are similarities between maximal surfaces and minimal surfaces, apart from being of zero mean curvature, for example and both admit the Weierstrass Enneper representation. However, striking differences emerge in the global study of these surfaces. While the only complete maximal surfaces are planes, there are many complete minimal surfaces apart from planes, such as the Catenoid, Enneper surface, Costa surfaces etc.

The global existence of maximal surfaces necessitates allowing natural singularities. We study a particular class of maximal surfaces called maxfaces, which were named by Umehara and Yamada in [13]. Maxfaces are those generalized maximal immersions that have only non-isolated singularities, and at singularities, limiting tangent vectors contain a light-like vector. The Lorentzian Catenoid is a maxface of genus zero. Imaizumi and Kato [10] classified genus-zero maxfaces. Kumar and Mohanty [12] have shown the existence of genus-zero maxfaces with an arbitrary number of complete and simple ends.

For higher genus surfaces, Kim and Yang [11] have proved the existence of genus one maxfaces and also shown the existence of maximal maps for higher genus surfaces. These maximal maps and maxfaces have two ends, both of which are catenoid types. Furthermore, Fujimori, Rossman, Umehara, Yang, and Yamada, [6], have constructed a family of complete maxfaces denoted as f_k , $k = 1, 2, 3, \dots$ with two ends. These maxface f_k is of genus k if k is odd and it has genus $\frac{k}{2}$ if k is even. All of them have two ends.

2020 *Mathematics Subject Classification.* 53A35.

Key words and phrases. Complete maxface, maximal map, maxface with Enneper end.

In 2016, authors of [5] constructed maxfaces of any odd genus g with two complete ends (if $g = 1$, the ends are embedded) and maxfaces of genus $g = 1$ with three complete embedded ends. Recently, Fujimori and Kaneda, [4], have demonstrated the existence of non-orientable higher genus maximal maps. In [13], Umehara and Yamada provided an example of a Lorentzian Chen–Gackstatter maxface, which is a genus one maxface with one Enneper end.

Here we focus on higher genus ($g \geq 2$) maxfaces with Enneper end and prove the existence of higher genus maxfaces with one Enneper end.

For constructing maxfaces of higher genus, the obvious initial approach is to consider companion surfaces. Suppose for a minimal surface the Weierstrass data on a Riemann surface M is $\{g, dh\}$. Then if the companion exists, the corresponding maxface would have the data $\{-ig, idh\}$. However, this approach faces two main challenges:

1. It is possible that the singularity set may extend towards the ends, preventing the creation of a complete maxface. For instance, consider the Weierstrass data for Jorge-Meek's minimal surface, given by:

$$g(z) = z^n \quad \text{and} \quad \omega = \frac{dz}{(z^{n+1} - 1)^2}.$$

This data results in a complete minimal surface on $\mathbb{C} \cup \{\infty\}$ with punctures $\{1, \zeta, \zeta^2, \dots, \zeta^{n-1}\}$, where $\zeta = \exp\left(\frac{2i\pi}{n}\right)$. It is observed that the companion whose Gauss map is $g_0 = -ig$ gives a maximal map, but it is not a complete maxface because the singular set $\{z \mid |g_0(z)| = 1\}$ is not compact. We refer to [13] for the definition of a complete maxface.

2. The second issue concerns the solvability of the period problem in a direct way. For example, consider the data for the Costa surface:

$$M = \{(z, w) \in \mathbb{C} \times \mathbb{C} \cup \{(\infty, \infty)\} \mid w^2 = z(z^2 - 1)\} \setminus \{(0, 0), (\pm 1, 0)\}$$

with data $\left\{ \frac{a}{w}, \frac{2a}{z^2 - 1} dz \right\}$, $a \in \mathbb{R}^+ \setminus \{0\}$.

Suppose there exists a maxface for which the companion is the Costa surface. Then the data should be $\{M, \frac{-ia}{w}, \frac{2ia}{z^2 - 1} dz\}$. Let τ be an one-sheeted loop around $(-1, 0)$ that does not contain $(1, 0)$. Then $\int_{\tau} \left(\frac{2ia}{z^2 - 1} dz \right) = 2ia$, $a \neq 0$. Therefore, for the corresponding maxface, the period problem is not solved. Hence, there does not exist any maxface for which the corresponding companion is the Costa surface.

Therefore, to construct a maxface, we usually set aside the companion and solve the period problem from scratch while keeping singularities in mind to ensure completeness. Using the method proposed by Wolf and Weber [14], [15], we prove the following:

Theorem 1.1. *For any genus p , a complete maxface of genus p with one Enneper-type end exists. Moreover,*

(1) this maxface has eight symmetries and

(2) *it is not the companion of the higher genus minimal surface as in [14] with Enneper ends.*

In the literature on the existence of maximal surfaces [6, 7, 11], we have primarily encountered the method of solving the period problem described in some articles [1, 8, 9] co-authored by Meeks. This method effectively reduces the period problem for many curves to just one or two curves, making it a valuable tool for constructing many minimal surfaces. However, in the case of maximal surfaces, most of the existing literatures have only managed to produce a maximum of two catenoid ends. In an ongoing work, the third author, with other collaborators [2] proved the existence of higher genus maxface and more than three catenoid or planar ends. But the case of Enneper ends was missing. Here we start from scratch, solve the period problem, and prove the existence of new maxfaces with one Enneper end.

We employ a method initiated by Weber and Wolf, [14], [15], to solve the period problem.

In Section 3, we recall the construction of minimal surfaces by zigzag, as presented in [14]. Using similar methods, in Proposition 3.1, we construct maxfaces with zigzag. We demonstrate that this maxface is not the companion of the minimal surface by zigzag; instead, it is symmetric to a companion of the same minimal surface.

Our goal is to construct maxfaces distinct from the companions of minimal surfaces by zigzag that are not symmetric to their companions. To achieve this, in Section 4, we introduce a geometric shape known as “tweezers” (a special ortho-disk in the terminology of [15]). In Theorem 5.1 we prove that for any genus $p \geq 2$, if there exists a reflexive tweezer, then there exists a maxface that is neither the companion of the minimal surface derived from the zigzag nor the companion of any symmetric minimal surface derived from the zigzag. Section 6 delves into a discussion regarding the existence of reflexive tweezers.

2. PRELIMINARIES

We recall the Weierstrass-Enneper representation for the minimal surfaces in \mathbb{R}^3 and maximal surfaces as well as maxfaces in the Lorentz Minkowski space \mathbb{E}_1^3 . Here \mathbb{E}_1^3 is the vector space \mathbb{R}^3 with the bilinear form $dx^2 + dy^2 - dz^2$.

2.1. Weierstrass-Enneper representation for minimal surfaces in \mathbb{R}^3 . For an oriented minimal surface $X : M \rightarrow \mathbb{R}^3$, there is a natural Riemann surface structure on M together with a meromorphic function g as well as a holomorphic one-form dh on M such that the poles and zeros of g match with the zeros of dh with the same order, and

$$(2.1) \quad X(p) = \operatorname{Re} X(x_0) + \operatorname{Re} \int_{x_0}^p \left(\frac{1}{2}(g^{-1} - g), \frac{i}{2}(g^{-1} + g), 1 \right) dh.$$

The triple $\{M, g, dh\}$ is referred to as the Weierstrass data for the minimal surface (X, M) . Furthermore, with such g and dh on a Riemann surface M , if the above integral is well defined, then it is a minimal immersion in \mathbb{R}^3 .

Now, let us move to the maximal immersions.

2.2. Weierstrass-Enneper representation for the maximal map. Let M be a Riemann surface, g a meromorphic function on M and dh a holomorphic 1-form on M , such that the following conditions are satisfied:

- (1) If $p \in M$ is a zero or pole of g of order m , then dh has a zero at p of order at least m ,
- (2) $|g|$ is not identically equal to 1 on M ,
- (3) for all closed loops γ on M ,

$$(2.2) \quad \int_{\gamma} g dh + \overline{\int_{\gamma} g^{-1} dh} = 0, \quad \operatorname{Re} \int_{\gamma} dh = 0.$$

Then the map $X : M \longrightarrow \mathbb{E}_1^3$ defined by

$$(2.3) \quad X(p) = \operatorname{Re} \int_{x_0}^p \left(\frac{1}{2}(g^{-1} + g), \frac{i}{2}(g^{-1} - g), 1 \right) dh$$

is a maximal map with the base point $x_0 \in M$ [3], [13]. Furthermore, any maximal map can be expressed in this form. The triple (M, g, dh) constitutes the Weierstrass data for the maximal map.

The pullback metric on the Riemann surface M is given by

$$ds^2 = \frac{1}{4} (|g|^{-1} - |g|)^2 |dh|^2,$$

and the singular locus of the maximal map with Weierstrass data (M, g, dh) is the subset $\{p \in M \mid |g(p)| = 1 \text{ or } dh(p) = 0\}$.

In the context of **maxfaces**, it is known that

$$(2.4) \quad (g)_0 - (g)_{\infty} = (dh)_0.$$

Therefore, the singular locus for the maxface is $\{p \in M \mid |g(p)| = 1\}$.

The completeness of a maxface can be determined using the following criterion:

Fact 2.1. *A maxface is complete (see [13, Corollary 4.8]) if and only if the following three hold:*

- (1) M is bi-holomorphic to $\overline{M} \setminus \{p_1, \dots, p_n\}$, where \overline{M} is a compact Riemann surface.
- (2) $|g| \neq 1$ at p_j , $1 \leq j \leq n$.
- (3) The induced metric ds^2 is complete at the ends.

3. MAXFACE WITH ENNEPER ENDS FROM A SYMMETRIC ZIGZAG

This section revisits the construction in [14] of a minimal surface using the zigzag method. Subsequently, we will determine the maxface that corresponds to this minimal surface as its companion. Furthermore, we will construct a maxface using the same zigzag approach and establish its relationship with the companion maxface.

3.1. Minimal surfaces by Weber and Wolf.

Definition 3.1 ([14]). *A zigzag Z of genus p is an open and properly embedded arc in \mathbb{C} composed of alternating horizontal and vertical subarcs with angles of $\frac{\pi}{2}, \frac{3\pi}{2}, \frac{\pi}{2}, \dots, \frac{3\pi}{2}, \frac{\pi}{2}$ between consecutive sides, and having $2p + 1$ vertices (there are $2p + 2$ sides, including an initial infinite vertical side and a terminal infinite horizontal side). A symmetric zigzag of genus p is a zigzag of genus p which is symmetric about the line $y = x$.*

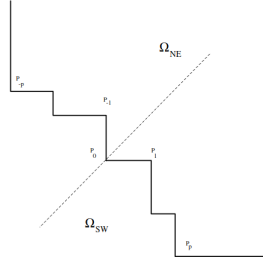


FIGURE 1. Zigzag of genus p (Picture Courtesy: Weber and Wolf [14])

A symmetric zigzag of genus p divides \mathbb{C} into two regions, one of which we call by the name Ω_{NE} and the other by Ω_{SW} (see Figure 1).

Definition 3.2. *A symmetric zigzag Z is called reflexive if there is a conformal map $\phi : \Omega_{NE}(Z) \rightarrow \Omega_{SW}(Z)$ which takes vertices to vertices.*

3.1.1. Construction of minimal surface. Let Z be the genus p reflexive zigzag separating \mathbb{C} into two regions namely Ω_{NE} and Ω_{SW} . We denote the vertices of Ω_{NE} by $\{P_j\}_{j=-p}^p$, $P_\infty = \infty$. The vertices of Ω_{SW} are labeled in the reverse order: $Q_j = P_{-j}$ for $j \in \{-p, -(p-1), \dots, p\}$ and $Q_\infty = \infty$. By doubling these two regions, we obtain two punctured spheres, denoted as S_{NE} and S_{SW} , each with $2p + 1$ marked points P_j and Q_j , respectively, as well as a puncture at P_∞ . Further, we take the hyperelliptic cover \mathcal{R}_{NE} (respectively, \mathcal{R}_{SW}) of S_{NE} (respectively, S_{SW}) branched at $\{P_j\}$ and (respectively, $\{Q_j\}$). respectively. Let

$$(3.1) \quad \pi_{NE} : \mathcal{R}_{NE} \rightarrow S_{NE} \quad \text{and} \quad \pi_{SW} : \mathcal{R}_{SW} \rightarrow S_{SW}$$

be the degree two branched covering maps. Since the zigzag Z is reflexive, a there is a conformal map $\phi : \Omega_{NE} \rightarrow \Omega_{SW}$ taking the vertices to vertices. This ϕ induces a conformal map

$$\tilde{\phi} : \mathcal{R}_{NE} \rightarrow \mathcal{R}_{SW}$$

such that $\tilde{\phi}(P_j) = Q_j$ for all j .

The flat metric $|dz|$ on Ω_{NE} extends to a singular flat metric on S_{NE} with cone angles at P_j . Its pullback through π_{NE} (see (3.1)) is a singular flat metric on \mathcal{R}_{NE} . The corresponding nonvanishing one form (see [14]) is denoted by ω_{NE} . Similarly, denote by ω_{SW} the nonvanishing one form induced on \mathcal{R}_{SW} by the flat metric $|dz|$ on Ω_{SW} .

We define two flat forms $\alpha = \exp(\frac{-\pi i}{4})\omega_{NE}$ and $\beta = \exp(\frac{-\pi i}{4})\tilde{\phi}^*\omega_{SW}$ on \mathcal{R}_{NE} . We choose c and define $dh = cd\pi_{NE}$ such that $\alpha\beta = dh^2$ (see [14] for the details).

Finally, we define $g = \frac{\alpha}{dh}$ and consider the formal Weierstrass data as $\{g, dh\}$. Weber and Wolf have proven in [14] that this pair gives the minimal surface by showing that

$$\int_{B_j} gdh = \int_{B_j} \alpha = \overline{\int_{B_j} g^{-1}dh} = \overline{\int_{B_j} \beta}$$

for all $\{B_{\pm j}\}_{j=1}^p$ (defined in the proof of [14, Theorem 3.3]). We will explain this technique more explicitly in the next section, where we will modify it to generate a maximal surface.

3.2. Maximal surface generated from zigzag. Using the terminology in Section 3.1, define two nonvanishing holomorphic one forms $\tilde{\alpha} = \exp(\frac{\pi i}{4})\omega_{NE}$ and $\tilde{\beta} = \exp(\frac{\pi i}{4})\tilde{\phi}^*\omega_{SW}$. By definition, B_j encloses exactly around the line segment $P_{j+1}P_j$ and B_{-j} encloses exactly around the line segment $P_{-j-1}P_{-j}$. Since ω_{NE}, ω_{SW} are flat forms,

$$\int_{B_j} \tilde{\alpha} = \exp(\frac{\pi i}{4}) \int_{B_j} \omega_{NE} = 2 \exp(\frac{\pi i}{4}) \int_{P_{j+1}}^{P_j} dz = 2 \exp(\frac{\pi i}{4})(P_j - P_{j+1}).$$

Similarly, for $\tilde{\beta}$,

$$\begin{aligned} \int_{B_j} \tilde{\beta} &= \exp\left(\frac{\pi i}{4}\right) \int_{\tilde{\phi}(B_j)} \omega_{SW} = 2 \exp\left(\frac{\pi i}{4}\right) \int_{Q_{j+1}}^{Q_j} dz \\ &= 2 \exp\left(\frac{\pi i}{4}\right) (Q_j - Q_{j+1}) = 2 \exp\left(\frac{\pi i}{4}\right) (P_{-j} - P_{-j-1}). \end{aligned}$$

By symmetry of zigzag, we have $-\overline{\exp(\frac{\pi i}{4})P_{-j}} = \exp(\frac{\pi i}{4})P_j$. Therefore, $-\overline{\int_{B_j} \tilde{\beta}} = \int_{B_j} \tilde{\alpha}$ for all B_j .

We define $\tilde{g} = \frac{\tilde{\alpha}}{\tilde{d}\tilde{h}}$, where $\tilde{d}\tilde{h} = \tilde{c}d\pi_{NE}$ for some \tilde{c} , such that $\tilde{\alpha}\tilde{\beta} = \tilde{d}\tilde{h}^2$. Therefore $\tilde{g}\tilde{d}\tilde{h} = \tilde{\alpha}$ and $\tilde{g}^{-1}\tilde{d}\tilde{h} = \tilde{\beta}$. Since $\tilde{d}\tilde{h}$ is an exact form, we deduce that $\int_{B_j} \tilde{d}\tilde{h} = 0$. Further from discussions in the last paragraph it is deduced that

$$\int_{B_j} \tilde{g}\tilde{d}\tilde{h} = -\overline{\int_{B_j} \tilde{g}^{-1}\tilde{d}\tilde{h}}$$

for all B_j . Further, since \tilde{g} has zero at P_∞ , the singularity set is compact. Thus we conclude the following:

Proposition 3.1. *The triple $\{\mathcal{R}_{NE} \setminus \{P_\infty\}, \tilde{g}, \tilde{d}\tilde{h}\}$ defines a maxface. This surface, which is denoted by \tilde{X} , has at most eight symmetries. Moreover, the following hold:*

- (1) *The minimal surface X is not the companion of \tilde{X} .*
- (2) *The companion of the minimal surface X exists; denote it by X_C . Then X_C and \tilde{X} are symmetric.*

Proof. It is easy to see that $\frac{\tilde{\alpha}}{\alpha} = \frac{\tilde{\beta}}{\beta} = i$. Therefore, $\frac{\tilde{\alpha}\tilde{\beta}}{\alpha\beta} = -1$. Thus,

$$\left\{ \frac{\tilde{d}\tilde{h}^2}{d\tilde{h}^2} = -1 \right\} \implies \{\tilde{d}\tilde{h} = idh\}.$$

Therefore, $\tilde{g} = \frac{i\alpha}{idh} = \frac{\alpha}{dh} = g$. Thus, the corresponding maximal surface has data (g, idh) . The minimal surface and the maximal surface share the same underlying Riemann surface, and they have at most eight conformal and anticonformal isometries.

Companion of X , which is denoted by X_C , is given by the Weierstrass data as $g_1 = -ig$ and $dh_1 = idh$, if period condition holds. We verify it here. Since dh is exact, we have $\int_{\gamma} dh_1 = 0$ for all $\gamma \in \{B_{\pm j}\}_{j=1}^p$. As $\int_{\gamma} gdh = \overline{\int_{\gamma} g^{-1}dh}$,

$$\int_{\gamma} g_1 dh_1 = \int_{\gamma} g dh = \overline{\int_{\gamma} g^{-1} dh} = -\overline{\int_{\gamma} g_1^{-1} dh_1}.$$

Thus, $\{g_1, dh_1\}$ is a Weierstrass data on \mathcal{R}_{NE} for the maximal surface.

We have

$$\tilde{X}(p) = \operatorname{Re} \int_0^p \left((g + \frac{1}{g}) \frac{idh}{2}, \frac{i}{2}(g - \frac{1}{g})idh, idh \right),$$

$$X_C(p) = \operatorname{Re} \int_0^p \left((g - \frac{1}{g}) \frac{dh}{2}, \frac{i}{2}(g + \frac{1}{g})dh, idh \right).$$

It is straightforward to check that $\tilde{X}(p) = \Psi(X_C(p))$ where $\Psi : \mathbb{E}_1^3 \rightarrow \mathbb{E}_1^3$ is the map defined by $(x, y, z) \mapsto (y, -x, z)$. Therefore, these two maximal surfaces are symmetric. \square

Similarly, one may attempt to construct minimal and maximal maps by zigzags symmetric about the line $y = -x$, but again, the surfaces turn out to be the same modulo symmetry.

4. TWEEZERS AND CORRESPONDING ZIGZAGS OF GENUS p

In this section, we will first revisit the concept of an "orthodisk" as described in [15]. We will then focus on a specific class of orthodisks, which we refer to as "tweezers". Although tweezers were inspired by "zigzags", they differ significantly in many aspects. We will explore the relationships between the Riemann surface associated with tweezers and \mathcal{R}_{NE} associated to zigzags.

4.1. Conformal polygon and orthodisk [15]. On the upper half-plane, consider $n \geq 3$ marked points $\{t_j\}_{j=1}^n$ lying on the real line. The point $t_\infty = \infty$ is also treated as one of these marked points. The upper half-plane equipped with these marked points is referred to as a conformal polygon, while the marked points are referred to as its vertices. Two conformal polygons are called equivalent under conformal mapping if there exists a biholomorphism of the upper half-plane that preserves the set of vertices while fixing the point ∞ .

Let $a_j, j \in \{1, \dots, n\} \cup \{\infty\}$, denote a set of odd integers such that

$$(4.1) \quad a_\infty = -4 - \sum_j a_j.$$

A vertex t_j is called "finite" if $a_j > -2$; otherwise, it is classified as "infinite". According to 4.1, there is at least one finite vertex, which may be coincide with t_∞ . We have the corresponding Schwarz–Christoffel map

$$F(z) := \int_i^z (t - t_1)^{\frac{a_1}{2}} \dots (t - t_n)^{\frac{a_n}{2}} dt$$

defined on the complement of the infinite vertices in the upper half-plane $\mathbb{H} \cup \mathbb{R}$.

Upper half plane, without the infinite vertices, equipped with the pullback, by F , of the flat metric on \mathbb{C} is called an orthodisk.

The integer a_j corresponds to cone angle of $\frac{a_j+2}{2}\pi$ at t_j . Negative angles bear significance, as a vertex with a negative angle $-\theta$ resides at infinity and represents the intersection of two lines. These lines also intersect at a finite point, forming a positive angle $+\theta$ at that intersection.

An orthodisk is called symmetric if it has a reflectional symmetry which fixes two vertices. Two orthodisks that share the same underlying conformal polygon, but having possibly different exponents, are called **conformal orthodisks**. Consider two orthodisks, X_1 and X_2 , each with distinct vertex data. These orthodisks are termed **conjugate** if there exists a straight line $l \subset \mathbb{C}$ such that the corresponding periods are symmetric with respect to l . Orthodisks X_1 and X_2 are called **reflexive** if they are both conformal and conjugate.

Below, we will discuss a particular type of ortho-disk, which we call tweezers.

4.2. Symmetric tweezers of genus p . A tweezer of genus p , with $p \geq 2$, is an open arc in \mathbb{C} consisting of $2p + 1$ vertices $\{P_j\}_{j=-p}^p$ and $2p + 2$ edges such that

- (1) the interior angle of the region that is left when we go from P_p to P_{-p} alternate between $\frac{3\pi}{2}, \frac{\pi}{2}$ except at $P_{\pm 1}, P_0$,
- (2) the interior angle at $P_{\pm 1}$ is always $\frac{\pi}{2}$, and
- (3) The interior angle at P_0 is $\frac{\pi}{2}$ when p is even and it is $\frac{3\pi}{2}$ when p is odd.

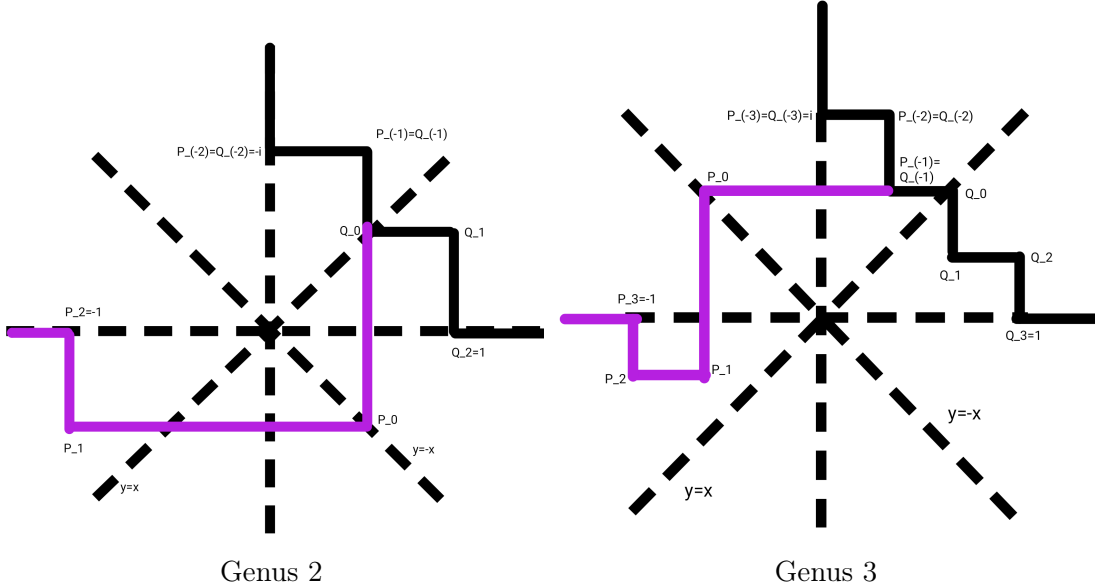


FIGURE 2. Symmetric tweezers and its corresponding zigzags genus two and genus three.

Moreover, at each vertex, there is an exterior angle assigned to it. If at P_k the interior angle as above is θ , then the corresponding exterior angle is $2\pi - \theta$. The notion of interior and exterior angles help us to recognize the image of \mathbb{H} under the Schwarz–Christoffel map, as discussed below. For two fixed set of real numbers $t_{-p} < \dots < t_p$, we will use the notation Ω_{Gdh} (following [15]) to mean $\mathbb{H} \cup \mathbb{R}$ with the flat metric induced by the unique Schwarz–Christoffel map taking \mathbb{H} to the interior of the polygon enclosed by the tweezer in the side of the interior angles such that the map sends \mathbb{R} to the tweezer and the point t_j to P_j . Similarly, for another set of real numbers $s_{-p} < \dots < s_p$ we can find a unique Schwarz–Christoffel map, sending \mathbb{H} to the interior polygon enclosed by the tweezer in the side of the exterior angle such that the image of s_j is P_{-j} which we call as Q_j . We call $\mathbb{H} \cup \mathbb{R}$ with the flat metric induced by this map as $\Omega_{G^{-1}dh}$. We write the Schwarz–Christoffel maps

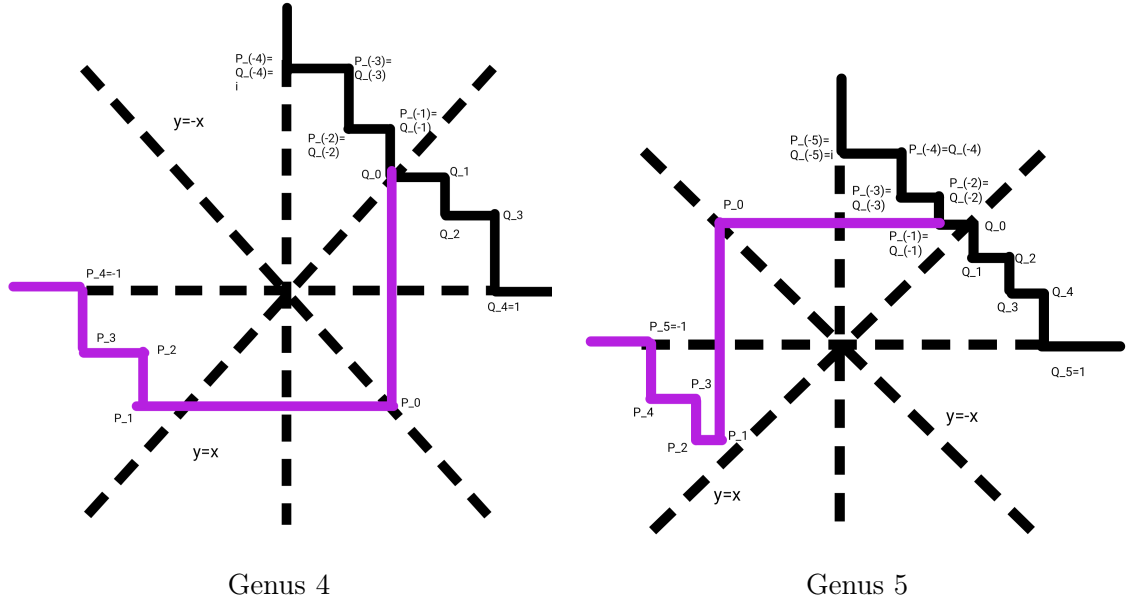


FIGURE 3. Symmetric tweezers and its corresponding zigzags genus 4 and genus 5

for the corresponding regions:

$$z^{-1} \longrightarrow \int_i^z \prod_{j=-p}^p (t - t_j)^{\frac{a_j}{2}} dt \quad \text{on } \Omega_{Gdh},$$

$$z^{-1} \longrightarrow \int_i^z \prod_{j=-p}^p (t - s_j)^{\frac{b_j}{2}} dt \quad \text{on } \Omega_{G^{-1}dh},$$

where

$$a_j = \begin{cases} \pm 1 & \text{alternatively when } j \neq \pm 1, 0, \\ -1 & \text{when } j = \pm 1, \\ 1 & \text{when } j = 0, p \text{ is odd,} \\ -1 & \text{when } j = 0, p \text{ is even,} \end{cases}$$

$$b_j = \begin{cases} \mp 1 & \text{alternatively when } j \neq \pm 1, 0, \\ 1 & \text{when } j = \pm 1, \\ -1 & \text{when } j = 0, p \text{ is odd,} \\ 1 & \text{when } j = 0, p \text{ is even.} \end{cases}$$

It is evident from our notation that the same convention used for naming vertices in the case of a zigzag has been applied to the vertices of the boundary of Ω_{Gdh} and

$\Omega_{G^{-1}dh}$. If we denote the vertices of Ω_{Gdh} as $\{P_j\}_{j=-p}^p$ with $P_\infty = \infty$, then we have chosen to name the vertices in the reverse order for $\Omega_{G^{-1}dh}$, i.e., the vertices are labeled as $Q_j = P_{-j}$ and $Q_\infty = \infty$

From a tweezer, we can obtain a zigzag by simply mapping the points of the tweezers P_j , where $j \geq 1$, to $-P_j$, P_0 to $-iP_0$ when p is even and P_0 to iP_0 when p is odd. Reversing the same process, we can get the corresponding tweezer from a given zigzag. For the case $p = 1$, the corresponding tweezer of genus 1 zigzag is just the rotation of the zigzag. Therefore, we skip the discussion of genus 1 tweezer except in some places where we need it. This zigzag may not necessarily be symmetric.

We call a tweezer symmetric if it is symmetric with respect to the line $y = -x$. It is clear that a zigzag that corresponds to a symmetric tweezer is symmetric along the line $y = x$.

Definition 4.1. *A symmetric tweezer is said to be reflexive if there is a conformal map $\phi : \Omega_{Gdh} \longrightarrow \Omega_{G^{-1}dh}$ taking vertices to vertices, i.e., $\phi(P_j) = Q_j$.*

In the context of an orthodisk, a tweezer gives rise to two orthodisks, denoted as Ω_{Gdh} with vertex data $\{t_j\}_{j=-p}^p$ and $\Omega_{G^{-1}dh}$ with vertex data $\{s_j\}_{j=-p}^p$. Here, t_j is mapped to P_j , and s_j is mapped to Q_j . For a symmetric tweezer, these two orthodisks are conjugate. Reflexivity implies that the corresponding conformal polygons are conformal.

4.3. Riemann surfaces from the tweezer. Similar to zigzags as in Section 3.1, we can construct first the punctured spheres $S_{\Omega_{Gdh}}, S_{\Omega_{G^{-1}dh}}$ with marked points $\{P_j\}_{j=-p}^p, \{P'_j = P_{-j}\}_{j=-p}^p$ with puncture $\{P_\infty = \infty\}$, and finally the hyperelliptic Riemann surfaces $\mathcal{R}_{Gdh}, \mathcal{R}_{G^{-1}dh}$ respectively, and if tweezer is reflexive, we get Riemann surfaces $\mathcal{R}_{Gdh}, \mathcal{R}_{G^{-1}dh}$ conformal taking corresponding Weierstrass's point to Weierstrass's points. We denote these Riemann surfaces as R_T . For given tweezer, we can construct the zigzag as discussed in the earlier subsection. Let for the corresponding zigzag, the marked sphere be S_Z with puncture $\{Q_\infty = \infty\}$, and the corresponding hyperelliptic Riemann surfaces be R_Z .

Proposition 4.1. *For a fixed genus $p \geq 2$, the Riemann surface R_T is neither conformal nor anticonformal to R_Z by a mapping that maps Weierstrass's points to Weierstrass's points. Here, T and Z denote the tweezer and its corresponding zigzag of genus p , respectively.*

Proof. Suppose there is a conformal or anticonformal map f between R_T and R_Z that takes corresponding Weierstrass points to each other, i.e., $f(W_T) = W_Z$ for Weierstrass points W_T on R_T and W_Z on R_Z . This means the marked sphere S_T maps to the marked sphere S_Z with $f(P_j) = Q_j, f(P_\infty) = Q_\infty$.

If f is conformal and it fixes at least 4 points on the real line, which are the Weierstrass points when we consider the restriction of f to the sphere S_T . In this

case, therefore, f would fix the entire real line, effectively taking tweezer T to the corresponding zigzag Z .

For the zigzag, the angle between two consecutive sides alternates, whereas for the tweezer when $p \geq 2$, this alternation will not always occur (as seen in the Figure 2, 3).

If p is even, taking a neighborhood \mathcal{U} containing the arc $P_{-2}P_{-1}P_0P_1P_2$, we would find that the restricted map f on \mathcal{U} should map this arc to the corresponding arc of the zigzag $Q_{-2}Q_{-1}Q_0Q_1Q_2$. However, the interior angles at P_{-1}, P_0, P_1 are $\frac{\pi}{2}, \frac{\pi}{2}, \frac{\pi}{2}$ respectively, while the corresponding angles at Q_{-1}, Q_0, Q_1 are $\frac{3\pi}{2}, \frac{\pi}{2}, \frac{3\pi}{2}$ respectively, which is impossible due to conformality. Thus, no such conformal f exists when p is even and $p \geq 2$.

For odd $p \geq 2$, considering a neighborhood \mathcal{V} containing the arc $P_{-3}P_{-2}P_{-1}P_0$, a similar comparison between the angles at P_{-2}, P_{-1} and their corresponding vertices in Z leads to a contradiction. Hence, no such f exists when p is odd.

If there is an anticonformal map with similar conditions, the arguments remain the same, concluding that no such anticonformal map exists for either even or odd $p \geq 2$. \square

In view of the above proposition, if we construct maxface and minimal surface, those will not be isometric to the one we get from the zigzags as in Section 3. In the next section, we will generate minimal and maximal surfaces using these tweezers, similar to the previous subsections.

5. MINIMAL SURFACE AND MAXIMAL SURFACE WITH TWEEZERS X_T AND \tilde{X}_T

Similar to the zigzag case as in the Section 3.1, we obtain non-vanishing holomorphic forms ω_{Gdh} and $\omega_{G^{-1}dh}$ on \mathcal{R}_{Gdh} and $\mathcal{R}_{G^{-1}dh}$ respectively. If we start from the reflexive tweezer T , the conformal map $\phi : \Omega_{Gdh} \rightarrow \Omega_{G^{-1}dh}$ can be extended to a map $\tilde{\phi} : \mathcal{R}_{Gdh} \rightarrow \mathcal{R}_{G^{-1}dh}$ — between the corresponding hyperelliptic Riemann surfaces — for which $\tilde{\phi}(P_j) = Q_j$ for all j . Define the following four holomorphic forms on \mathcal{R}_{Gdh} :

$$\begin{aligned} \alpha &= \exp\left(-\frac{\pi i}{4}\right)\omega_{Gdh}, \\ \beta &= \exp\left(-\frac{\pi i}{4}\right)\tilde{\phi}^*(\omega_{G^{-1}dh}), \\ \tilde{\alpha} &= \exp\left(\frac{\pi i}{4}\right)\omega_{Gdh}, \\ \tilde{\beta} &= \exp\left(\frac{\pi i}{4}\right)\tilde{\phi}^*(\omega_{G^{-1}dh}). \end{aligned}$$

Using the relationship between the cone angles and the order of the zeros of the 1-forms, we find the divisors corresponding to these forms:

$$(\alpha) = (\tilde{\alpha}) = \begin{cases} P_{\pm p}^2 P_{\pm(p-2)}^2 \cdots P_{\pm 3}^2 P_0^2 P_{\infty}^{-2} & \text{if } p \text{ is odd} \\ P_{\pm p}^2 P_{\pm(p-2)}^2 \cdots P_{\pm 2}^2 P_{\infty}^{-2} & \text{if } p \text{ is even} \end{cases}$$

$$(\beta) = (\tilde{\beta}) = \begin{cases} P_{\pm(p-1)}^2 P_{\pm(p-3)}^2 \cdots P_{\pm 2}^2 P_{\pm 1}^2 P_{\infty}^{-4} & \text{if } p \text{ is odd} \\ P_{\pm(p-1)}^2 P_{\pm(p-3)}^2 \cdots P_{\pm 3}^2 P_{\pm 1}^2 P_0^2 P_{\infty}^{-4} & \text{if } p \text{ is even} \end{cases}$$

It is important to highlight that we use multiplicative notation for the divisor, while addition and subtraction follow the conventional complex number operations.

The differential of the holomorphic covering π_{Gdh} (branched at P_j) has the following divisor:

$$(d\pi_{Gdh}) = P_{\pm p}^1 P_{\pm(p-1)}^1 \cdots P_0^1 P_{\infty}^{-3}.$$

The quadratic differentials $\alpha\beta$ and $d\pi_{Gdh}^2$ share an identical set of zeros and poles, as do $\tilde{\alpha}\tilde{\beta}$. Consequently, there exist appropriate constants c and \tilde{c} such that: $\alpha\beta = (dh)^2$, where $dh = cd\pi_{Gdh}$ and $\tilde{\alpha}\tilde{\beta} = (\tilde{dh})^2$, where $\tilde{dh} = \tilde{c}d\pi_{Gdh}$

Now, we define the following formal Weierstrass data for our minimal surface and maximal maps:

$$\left(G_T = \frac{\alpha}{dh}, dh \right) \text{ for the minimal surface,}$$

$$\left(\tilde{G}_T = \frac{\tilde{\alpha}}{\tilde{dh}}, \tilde{dh} \right) \text{ for the maximal surface.}$$

Note that the divisor condition, as in the Equation 2.4, is trivially satisfied since at each zero and pole of G_T and \tilde{G}_T , there exists a zero of $d\pi_{Gdh}$ with an equal order.

The period problem can be resolved using the same technique as discussed in Section 3.2. We begin with the basis of homology, denoted as $H_1(\mathcal{R}_{Gdh}, \mathbb{Z})$. For $j = -p, \dots, p-1$, let B_j represent the loop in $S_{\Omega G_{dh}}$ that encloses only the line segment $P_j P_{j+1}$ within the disk and no other vertices in its interior. These curves have closed lifts \tilde{B}_j to \mathcal{R}_{Gdh} and form a homology basis of \mathcal{R}_{Gdh} . The following statements are valid:

$$\begin{aligned}
\int_{\widetilde{B}_j} \alpha &= 2 \exp\left(-\frac{\pi i}{4}\right) (P_j - P_{j+1}) \\
\int_{\widetilde{B}_j} \beta &= 2 \exp\left(-\frac{\pi i}{4}\right) (P_{-j} - P_{-j-1}) \\
\int_{\widetilde{B}_j} \tilde{\alpha} &= 2 \exp\left(\frac{\pi i}{4}\right) (P_j - P_{j+1}) \\
\int_{\widetilde{B}_j} \tilde{\beta} &= 2 \exp\left(\frac{\pi i}{4}\right) (P_{-j} - P_{-j-1}).
\end{aligned}$$

Due to the symmetry of the tweezers, we can further deduce that

$$(5.1) \quad \int_{\widetilde{B}_j} \alpha = \overline{\int_{\widetilde{B}_j} \beta}$$

$$(5.2) \quad \int_{\widetilde{B}_j} \tilde{\alpha} = -\overline{\int_{\widetilde{B}_j} \tilde{\beta}}.$$

Moreover as dh and \widetilde{dh} are exact, therefore for all loops $\int_{\widetilde{B}_j} dh = \int_{\widetilde{B}_j} \widetilde{dh} = 0$. Thus, equations (5.1) and (5.2) confirm that the following maps are minimal and maximal, respectively:

$$(5.3) \quad X_T(z) = \operatorname{Re} \int_0^z \left((G_T^{-1} - G_T) \frac{dh}{2}, i(G_T^{-1} + G_T) \frac{dh}{2}, dh \right)$$

$$(5.4) \quad \tilde{X}_T(z) = \operatorname{Re} \int_0^z \left((\tilde{G}_T^{-1} + G_T) \frac{\widetilde{dh}}{2}, i(\tilde{G}_T^{-1} - \tilde{G}_T) \frac{\widetilde{dh}}{2}, \widetilde{dh} \right).$$

We have the following theorem

Theorem 5.1. *Given a reflexive tweezer T of genus p , there exist a minimal surface X_T and a maxface \tilde{X}_T of genus p , each having one Enneper end and at most eight symmetries. Furthermore, X_T (respectively, \tilde{X}_T) is not symmetric to the minimal surface X (respectively, \tilde{X}) as discussed in Section 3.*

Proof. Equation (5.3) defines the minimal surface, and Equation (5.4) defines the corresponding maximal map.

As we have already established the divisor condition, as in Equation (2.4), it follows that the maximal map given in Equation (5.4) indeed represents a maxface.

Concerning completeness, we first observe that at the end of the maxface, the Gauss map has a zero. Consequently, the singular set $\{p : |\tilde{G}_T(p)|=1\}$ is compact. Furthermore, we can confirm that the metric is complete at the end of both X_T and \tilde{X}_T since the data at the end is the same as the data for the Enneper end.

The remaining task involves proving that the minimal surface X_T is not symmetric to the minimal surface X . If such symmetry existed, there would either be a conformal or anticonformal diffeomorphism between the corresponding Riemann surfaces. However, as stated in Proposition 4.1, this is not possible. \square

6. EXISTENCE OF A REFLEXIVE TWEEZER

In this section, we will demonstrate the existence of a reflexive tweezer. The proof closely follows the approach used for the zigzag case, as detailed in Section 5 of [14]. While we could have directly stated the existence of the tweezer as a corollary of the zigzag and orthodisks case, we choose to present it here for the sake of clarity and comprehensiveness. Therefore, the content presented below does not introduce new concepts; instead, it serves as an application of the arguments found in various works by Weber and Wolf. Consequently, we aim to emphasize several key points within the context of tweezers, and we will discuss these in the following subsections.

6.1. Space of Tweezers \mathcal{T}_p . Two symmetric tweezers of genus p , denoted as T and T' , are considered equivalent if the corresponding pairs of regions $(\Omega_{Gdh}^T, \Omega_{G^{-1}dh}^T)$ and $(\Omega_{Gdh}^{T'}, \Omega_{G^{-1}dh}^{T'})$ are conformal by a map that takes each vertex to the same vertex. Let \mathcal{T}_p denote the class of equivalent symmetric tweezers of genus p . Furthermore, there always exists a conformal map of \mathbb{C} that carries any symmetric tweezer to a symmetric tweezer t_0 , such that the two endpoints P_{-p} and P_p are i and -1 respectively, and $P_k = -i\overline{P_{-k}}$. From now onwards, we will represent a class of tweezer $[T] \in \mathcal{T}_p$ by the corresponding tweezer t_0 in $[T]$, unless stated otherwise.

Similar to the space \mathcal{Z}_p as defined in [14], we define a map

$$\mathcal{T}_p : \mathcal{T}_p \longrightarrow \mathbb{C}^{p-1}$$

as follows:

$$\mathcal{T}_p([t_0]) = (P_1(t_0), \dots, P_{p-1}(t_0)).$$

This map induces a topology on \mathcal{T}_p , making it homeomorphic to a $(p-1)$ -cell.

6.2. Height function, Sufficient condition of the reflexive Tweezers, and its properness. We will follow Subsection 4.2 of [14] in the present context. Consider the $2(p+1)$ -pointed sphere $S_{\Omega_{Gdh}}$ with marked points $P_{-p}, \dots, P_0, \dots, P_p$, and P_∞ . Remarkably, $S_{\Omega_{Gdh}}$ exhibits two distinct reflective symmetries: one related to the image of T , and another arising from a corresponding symmetry of the tweezer.

We denote $[C_k]$ the homotopy class of simple curves that encircle the points P_k and P_{k+1} for $k = 1, \dots, p-1$. Similarly, $[C_{-k}]$ is the homotopy class of simple curves enclosing the points P_{-k} and P_{-k-1} for $k = 1, \dots, p-1$. Furthermore, we define $[\alpha_k]$ as the combined pair of classes $[C_k] \cup [C_{-k}]$.

From the homotopy class of mappings that connect $S_{\Omega_{Gdh}}$ to $S_{\Omega_{G^{-1}dh}}$ (while preserving each of the vertices), we derive corresponding homotopy classes of curves on

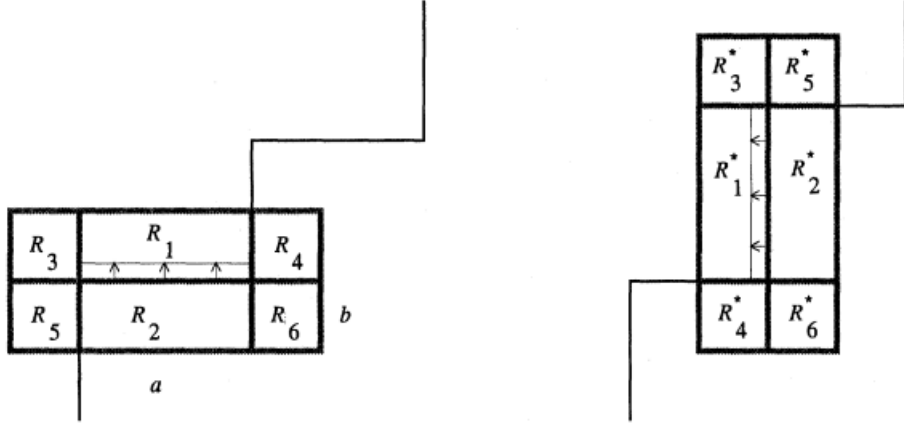


FIGURE 4. Picture from the Section 5.3.1 [15]

$S_{\Omega_{G^{-1}dh}}$, which are also denoted by $[\alpha_k]$. Additionally, we denote

$$E_{\Omega_{Gdh}}(k) := \text{Ext}_{S_{\Omega_{Gdh}}}([\alpha_k]) \quad \text{and} \quad E_{\Omega_{G^{-1}dh}}(k) := \text{Ext}_{S_{\Omega_{G^{-1}dh}}}([\alpha_k]),$$

representing the extremal lengths of $[\alpha_k]$ within the domains of $S_{\Omega_{Gdh}}$ and $S_{\Omega_{G^{-1}dh}}$ respectively.

Motivated by Definition 4.4 of [14], we construct the similar height function

$$D^T : \mathcal{T}_p \longrightarrow \mathbb{R}$$

defined by

$$(6.1) \quad D^T(T) = \sum_{j=1}^{p-1} \left(\exp \left(\frac{1}{E_{\Omega_{Gdh}}(j)} \right) - \exp \left(\frac{1}{E_{\Omega_{G^{-1}dh}}(j)} \right) \right)^2 + \sum_{j=1}^{p-1} (E_{\Omega_{Gdh}}(j) - E_{\Omega_{G^{-1}dh}}(j))^2$$

From the same argument as in the case of zigzag (see [14, Section 4.3]) it is clear that $D^T(T) = 0$ if and only T is reflexive. Moreover the properness of D^T is a direct consequence of Lemma 4.7.1, and Lemma 4.7.2 of [15].

6.3. Tangent vector at $t_0 \in \mathcal{T}$. Let us fix an edge E that is horizontal; the symmetric tweezer will give the corresponding edge E^* , which is vertical. For given b, δ , take maps f_ϵ^E and $f_{\epsilon^*}^E$ as in [15, (5.1)(a)] and [15, (5.1)(b)] respectively. Geometrically, these maps push the horizontal and vertical edges so that after applying both maps, the tweezer structure is preserved (see Figure 4). Under the reflection across the line $y = -x$, the region R_i is mapped to the region R_i^* as in figure 4.

We call the map $f_\epsilon^E \circ f_{\epsilon^*}^E$ above the “pushing out and pulling in” map for the edge E .

Let $\nu_\epsilon := \frac{(f_\epsilon)\bar{z}}{(f_\epsilon)_z}$ represents the Beltrami differential of f_ϵ , and define $\dot{\nu} = \frac{d}{d\epsilon}|_{\epsilon=0} \nu_\epsilon$. Similarly, let $\dot{\nu}^*$ denote the infinitesimal Beltrami differential of f_ϵ^* . Expressions for $\dot{\nu}$ and $\dot{\nu}^*$ are given in [15, (5.1)(a)] and [15, (5.1)(b)] respectively.

We take $\dot{\mu} = \dot{\nu} + \dot{\nu}^*$. This is a Beltrami differential supported on a bounded domain in $\mathbb{C} = \Omega_{Gdh} \cup t_0 \cup \Omega_{G^{-1}dh}$. Thus, this pair of Beltrami differentials lifts to a pair

$$(6.2) \quad \dot{\mu} = (\dot{\mu}_{\Omega_{Gdh}}, \dot{\mu}_{\Omega_{G^{-1}dh}})$$

on the pair $S_{\Omega_{Gdh}}$ and $S_{\Omega_{G^{-1}dh}}$.

The above defined $\dot{\mu}$ represents a tangent vector to \mathcal{T}_p at t_0 . The above process will yield different tangent vectors for different “pushing out and pulling in” maps.

6.4. Derivative of Extremal length function, and corresponding Quadratic Differential. Let Φ_k represent the quadratic differential associated with the homotopy class of curve α_k , defined as

$$\Phi_k := \frac{1}{2} d \operatorname{Ext}([\alpha_k])|_{\Omega_{Gdh}} \quad \text{and,}$$

$$(6.3) \quad (d \operatorname{Ext}([\alpha_k])|_{\Omega_{Gdh}}) [\widehat{\nu}] = 4 \operatorname{Re} \int_{\Omega_{Gdh}} \Phi_k \widehat{\nu}.$$

The horizontal foliation of Φ_k comprises curves connecting the same edges, as C_k , within Ω_{Gdh} . Furthermore, it preserves the reflective symmetry of the element in \mathcal{T}_p . Consequently, these foliations must either run parallel to or be perpendicular to the fixed sets of reflections (which correspond to the tweezer). Here, we are using the same notation for the foliation Φ_k both on the marked sphere $S_{\Omega_{Gdh}}$ and on Ω_{Gdh} .

Consider the edge E connecting vertices v_1 and v_2 , but $v_i \neq P_0$. Let Φ_k denote the quadratic differential corresponding to the homotopy class of curve C_k containing both v_1 and v_2 . Since genus $p \geq 2$, in this context, there is such an edge for which one of the following conditions holds for vertex v_i :

- (1) The orthodisk has an angle of $\frac{\pi}{2}$ at v_i .
- (2) Vertex v_i lies at infinity.
- (3) The orthodisk has an angle of $\frac{3\pi}{2}$ at v_i , and the foliation Φ_k is either parallel or orthogonal to the edges incident to v_i .

Using Proposition 5.3.2 from [15] we conclude that the holomorphic quadratic differential Φ_k is admissible on the edge corresponding to points v_1 and v_2 .

In the next subsection, we will select edge E such that the corresponding foliation is admissible on E . Additionally, we will consider the tangent vector $\dot{\mu}$ as described in (6.2), which we obtain by applying corresponding pushing out and pulling in function $f_\epsilon^E \circ f_{\epsilon^*}^E$ to the tweezer. Without loss of generality, we can select the edge corresponding to P_{-1} and P_{-2} .

6.5. Reflexive tweezer. Since the holomorphic quadratic differential Φ_k is admissible for the edge we selected (as demonstrated in the previous subsection), we can apply Lemma 5.3.1 from [15], leading to the following corollary for the tweezer case:

Corollary 6.1. *The expression $\operatorname{sgn}(\Phi_k \dot{\mu}_{\Omega_{Gdh}}(q))$ maintains a constant sign for $q \in E$, which is opposite to $\operatorname{sgn}(\Phi_k \dot{\mu}_{\Omega_{G^{-1}dh}}(q))$. Consequently,*

$$\operatorname{sgn}(d\operatorname{Ext}_{\Omega_{Gdh}}([\alpha_k])[\dot{\mu}_{\Omega_{Gdh}}]) = -\operatorname{sgn}(d\operatorname{Ext}_{\Omega_{G^{-1}dh}}([\alpha_k])[\dot{\mu}_{\Omega_{G^{-1}dh}}]).$$

In the above, we are employing the same notation (a slight abuse of notation) for the curve α_k in both Ω_{Gdh} and $\Omega_{G^{-1}dh}$, as well as the same symbol for the corresponding horizontal foliation.

Above corollary 6.1 is the main result that enables us to use the findings of zigzag, as presented in Section 5.3 of [14]. Since the proof is identical, we can establish the following fact:

Suppose there is a reflexive tweezers of genus $p - 1$, then there is a path (one dimensional real analytic manifold) $\mathcal{Y} \subset \mathcal{T}_p$ for which $\operatorname{Ext}_{\Omega_{Gdh}}(\alpha_i) = \operatorname{Ext}_{\Omega_{G^{-1}dh}}(\alpha_i)$ holds for $i = 2 \dots p - 1$.

If we restrict D^T as in the Equation (6.1) to \mathcal{Y} , we have

$$D^T|_{\mathcal{Y}} = \left(\exp\left(\frac{1}{\operatorname{E}_{\Omega_{Gdh}}(1)}\right) - \exp\left(\frac{1}{\operatorname{E}_{\Omega_{G^{-1}dh}}(1)}\right) \right)^2 + (\operatorname{E}_{\Omega_{Gdh}}(1) - \operatorname{E}_{\Omega_{G^{-1}dh}}(1))^2$$

We denote the above-restricted function by the same D^T . Moreover let $t_0 \in Y$, and let $\dot{\mu} \in T_{t_0} \mathcal{Y}$ corresponding to the edge we selected. We get

$$\begin{aligned} dD_{t_0}^T[\dot{\mu}] &= 2 \left(\exp\left(\frac{1}{\operatorname{Ext}_{\Omega_{Gdh}}([\alpha_1])}\right) - \exp\left(\frac{1}{\operatorname{Ext}_{\Omega_{G^{-1}dh}}([\alpha_1])}\right) \right) \\ &\quad \left(-\exp\left(\frac{1}{\operatorname{Ext}_{\Omega_{Gdh}}([\alpha_1])}\right) (\operatorname{Ext}_{\Omega_{Gdh}}([\alpha_1]))^{-2} d\operatorname{Ext}_{\Omega_{Gdh}}([\alpha_1])[\dot{\mu}_{\Omega_{Gdh}}] \right. \\ &\quad \left. + \exp\left(\frac{1}{\operatorname{Ext}_{\Omega_{G^{-1}dh}}([\alpha_1])}\right) (\operatorname{Ext}_{\Omega_{G^{-1}dh}}([\alpha_1]))^{-2} d\operatorname{Ext}_{\Omega_{G^{-1}dh}}([\alpha_1])[\dot{\mu}_{\Omega_{G^{-1}dh}}] \right) \\ &\quad + 2 (\operatorname{Ext}_{\Omega_{Gdh}}([\alpha_1]) - \operatorname{Ext}_{\Omega_{G^{-1}dh}}([\alpha_1])) (d\operatorname{Ext}_{\Omega_{Gdh}}([\alpha_1])[\dot{\mu}_{\Omega_{Gdh}}] - d\operatorname{Ext}_{\Omega_{G^{-1}dh}}([\alpha_1])[\dot{\mu}_{\Omega_{G^{-1}dh}}]) \end{aligned}$$

If we begin with $t_0 \in Y$ such that $D^T(t_0) \neq 0$ and choose $\dot{\mu}$ as described in 6.2 for the edge we selected at the beginning of this subsection. The equation above implies that $dD_{t_0}^T[\dot{\mu}] \neq 0$. However, since D^T is a proper map, it must have a critical point in the smooth manifold \mathcal{Y} ; therefore, at this critical point t_0 , we must have $D^T(t_0) = 0$.

Now, finally, we prove that for every genus p , there exists a reflexive tweezer using an induction argument as outlined in [14] (page 1165). To apply the induction argument for the case when $p = 1$, it is evident that both the Riemann surfaces resulting from the zigzag and the tweezer are square tori. Therefore, for $p = 1$, the

existence of reflexive zigzag and tweezer is immediate, and then we can proceed with the induction argument.

7. CONCLUDING REMARKS

We present new examples of maxfaces with one Enneper end. Furthermore, from the proof, it becomes evident that by suitably adjusting the orthodisk, we can effectively address the period problem associated with these maxfaces. However, there are two crucial aspects that this article does not cover, but are essential to explore:

Firstly, due to the lack of control over the modulus of the Schwarz–Christoffel map, we are uncertain about the precise nature of the singular set. Additionally, if we somehow manage to identify the singular set, we still need to determine the types of singularities that these maxfaces can exhibit. It is our hope that numerical analysis of the generic Schwarz–Christoffel map may yield some insights in this regard.

Secondly, as observed from the proof, the process involves defining the orthodisk in a suitable manner from the tweezers and then establishing the existence of a reflexive tweezer. A similar construction approach can be applied to obtain maxfaces corresponding to structures such as Costa Towers, $DH_{m,n}$ as discussed in [15]. This will remove scarcity of maxface with more number of ends.

The investigation of these two important aspects holds promise for advancing our understanding of maxfaces and their properties.

REFERENCES

- [1] M. Callahan, D. Hoffman, and W.H. Meeks III, *Embedded minimal surfaces with an infinite number of ends*, Invent. Math. **96** (1989), no. 3, 459–505. MR996552
- [2] H. Chen, A. Dhochak, P. Kumar, and S.R.R. Mohanty, *Higher genus embedded (in wider sense) maxfaces*, Under Preparation.
- [3] F. J. M. Estudillo and A. Romero, *Generalized maximal surfaces in lorentz–minkowski space l^3* , Mathematical Proceedings of the Cambridge Philosophical Society **111** (1992), no. 3, 515–524.
- [4] S. Fujimori and S. Kaneda, *Higher genus nonorientable maximal surfaces in the Lorentz–Minkowski 3-space*, Tohoku Mathematical Journal **75** (2023), no. 1, 1–14.
- [5] S. Fujimori, S. G. Mohamed, and M. Pember, *Maximal surfaces in Minkowski 3-space with non-trivial topology and corresponding CMC 1 surfaces in de Sitter 3-space*, Kobe J. Math. **33** (2016), no. 1-2, 1–12. MR3642418
- [6] S. Fujimori, W. Rossman, M. Umehara, K. Yamada, and S.-D. Yang, *New maximal surfaces in minkowski 3-space with arbitrary genus and their cousins in de sitter 3-space*, Results in Mathematics **56** (2009), no. 1, 41.
- [7] S. Fujimori, K. Saji, M. Umehara, and K. Yamada, *Singularities of maximal surfaces*, Mathematische Zeitschrift **259** (2007), no. 4, 827.
- [8] D. Hoffman and W. H. Meeks III, *Embedded minimal surfaces of finite topology*, Annals of Mathematics (1990), 1–34.

- [9] W. H. Meeks III and G. Tinaglia, *Triply periodic constant mean curvature surfaces*, Advances in Mathematics **335** (2018), 809–837.
- [10] T. Imaizumi and S. Kato, *Flux of simple ends of maximal surfaces in $R^{2,1}$* , Hokkaido Math. J. **37** (2008), no. 3, 561–610.
- [11] W. Kim and S.-D. Yang, *A family of maximal surfaces in lorentz-minkowski three-space*, Proceedings of the American Mathematical Society **134** (2006), no. 11, 3379–3390.
- [12] P. Kumar and S. R. R. Mohanty, *Genus zero complete maximal maps and maxfaces with an arbitrary number of ends*, to appear in Comptes Rendus- Serie Mathematique (2023), available at [arXiv:2306.09227](https://arxiv.org/abs/2306.09227).
- [13] M. Umehara and K. Yamada, *Maximal surfaces with singularities in minkowski space*, Hokkaido Mathematical Journal **35** (2006), no. 1, 13–40.
- [14] M. Weber and M. Wolf, *Minimal surfaces of least total curvature and moduli spaces of plane polygonal arcs*, Geometric And Functional Analysis GAFA **8** (1998).
- [15] ———, *Teichmuller theory and handle addition for minimal surfaces*, Annals of Mathematics **156** (1998), 713–795.

DEPARTMENT OF MATHEMATICS, SHIV NADAR INSTITUTE OF EMINENCE, DEEMED TO BE UNIVERSITY, DADRI 201314, UTTAR PRADESH, INDIA.

Email address: `rb212@snu.edu.in`

DEPARTMENT OF MATHEMATICS, SHIV NADAR INSTITUTE OF EMINENCE, DEEMED TO BE UNIVERSITY, DADRI 201314, UTTAR PRADESH, INDIA.

Email address: `indranil.biswas@snu.edu.in, inrdranil29@gmail.com`

DEPARTMENT OF MATHEMATICS, SHIV NADAR INSTITUTE OF EMINENCE, DEEMED TO BE UNIVERSITY, DADRI 201314, UTTAR PRADESH, INDIA.

Email address: `pradip.kumar@snu.edu.in`